Physics – Uspekhi **44** (10) 1061 – 1073 (2001)

FROM THE CURRENT LITERATURE

PACS numbers: 12.20.Fv, **42.50. – p**, **42.55. – f**, **42.65. – k**, 42.68.Wt

Optics of microdroplets

V V Datsyuk, I A Izmaĭlov

DOI: 10.1070/PU2001v044n10ABEH001018

Contents

Abstract. An overview of optical effects in micrometer-sized droplets is presented. The fundamentals of microdroplet optics are expounded. The scope of the analyzed phenomena includes enhancement of the spontaneous emission probability, laser generation, Raman light scattering, changes in the rates of physicochemical processes, and peculiarities of action on droplets by high-power light pulses. It is emphasized that the knowledge acquired can be applied to droplet structure analysis based on the measurement of resonance positions and amplitudes in elastic or inelastic light scattering spectra.

1. Introduction

Investigations into finely dispersive heterophase media such as aerosols, suspensions, gases and plasmas involving clusters are of great interest for both the development of new technologies and the cognition of anomalous physical phenomena [1 – 15]. Indeed, the rates of the elementary physicochemical processes in dispersive media are subject to variations which can be as great as to give rise to new physical objects with specific properties. For example, Smirnov and Eletskiĭ [10 – 12] detail the cluster plasma concept. The present review is focused on peculiar features of optical processes in microdroplets.

The optics of microdroplets has a long history. A review of research in this field may be started with a reference to a work of R Descartes published in 1639 [16]. It elaborated the ray theory of the refraction and reflection of light in an isolated spherical droplet. Two centuries later, G Airy improved this theory taking into consideration diffraction of light [17] (see also Ref. [18]). The importance of the matter can be illustrated by the following facts. On the one hand, Descartes resolved the light scattering problem soon after he had created analytical geometry [19]. On the other hand, modern authors [20 – 27] seek to find the solution of the same problem in the framework of geometrical (ray) optics.

A strict analytical solution to the problem of electromagnetic wave scattering from the homogeneous sphere of an arbitrary radius and with arbitrary dielectric constant was independently obtained by Lorenz [28], Mie [29], Debye [30], and Love [31] (see also Refs [18, 32, 33]). At about the same time, Lord Rayleigh studied sound propagation over a curved gallery surface [34]. This work of Rayleigh deserves to be mentioned here since the term 'whispering gallery modes' (WGM) is also frequently used with reference to electromagnetic surface oscillations in optical resonators.

For an appreciable length of time, light scattering by droplets had been a matter of purely academic interest. The situation drastically changed in the mid-1980s in connection with the appearance of lasers and computing machines. Microdroplet studies were reported in hundreds of experimental and theoretical works, and their results found application in various branches of technology. The understanding of optical processes achieved in the course of these studies gave rise to new branches of applied physics [35 – 44]. For example, Braginsky et al. [36, 37] considered the possibility of using WGM in solid-state microresonators for the construction of a Feynman quantum-mechanical computer. In paper [44], a quantum-dot laser scheme was proposed.

The present review will consider various WGM properties in droplets, observable subject to the applicability of the Lorenz – Mie theory.

Light scattering by an isolated droplet is usually referred to as Mie scattering provided the dimensionless droplet radius

V V Datsyuk Taras Shevchenko Kiev National University, Physics Department, Vladimirskaya ul. 64, 01033 Kiev, Ukraine
Tel. (038-044) 266-44 77. E-mail: datsyuk@ups.kiev.ua
I A Izmaĭlov Institute of Semiconductor Physics, National Academy of Sciences of the Ukraine, prosp. Nauki 45, 03028 Kiev, Ukraine
Tel. (038-044) 265-77 78

Received 22 May 2001
Uspekhi Fizicheskikh Nauk **171** (10) 1117 – 1129 (2001)
Translated by Yu V Morozov; edited by A Radzig

ranges from a few tens to several hundreds, namely

$$x \equiv \frac{2\pi a}{\lambda} \simeq 10^2 .$$

From here on, λ is the light wavelength in the medium surrounding the droplet, and a is the droplet radius. If λ lies in the visible range, then a measures a few tens of micrometers. (When $x \ll 1$, the light scattering is called Rayleigh scattering [45]).

2. Mie scattering

The formalism employed in the solution to the problem of scattering of the plane monochromatic wave by a ball is termed the Lorenz–Mie theory; detailed characteristic of it can be found in monographs [32, 46] (see also [47]). It is described in brief below. Such a description of the theoretical model is deemed necessary not only for the calculation of scattered radiation parameters. In what follows, it will be shown that excitation of WGM results in the formation of resonance structures both in the scattered light spectra and in spontaneous radiation spectra.

In the framework of classical electrodynamics, vectors of the electric field strength **E** and the magnetic field strength **H** can be expressed through the Debye electric and magnetic potentials v^p. Hereinafter, the superscript p is used to indicate the polarization of electromagnetic fields. Let $p = 0$ for a transverse electric (TE) type field, and $p = 1$ for a transverse magnetic (TM) type field. The Debye potentials v^p satisfy the scalar wave equation

$$\Delta v^p + \frac{\varepsilon\mu}{c^2}\,\frac{\partial^2}{\partial t^2}\, v^p = 0 , \tag{1}$$

where Δ is the Laplace operator, $\partial/\partial t$ denotes the time derivative, and c is the velocity of light in a vacuum. It is assumed that the dielectric and magnetic permittivities of the ball (II) and the surrounding medium (I) are constant:

$$\varepsilon = \begin{cases} \varepsilon^{(\mathrm{II})}, & r \leqslant a, \\ \varepsilon^{(\mathrm{I})}, & r > a, \end{cases} \qquad \mu = 1 .$$

Here r is the distance from the center of the ball. The relative index of light refraction

$$n = \sqrt{\frac{\varepsilon^{(\mathrm{II})}}{\varepsilon^{(\mathrm{I})}}} .$$

The general solution of Eqn (1) in the spherical system of coordinates r, θ, ϕ at $r \leqslant a$ may be represented in the form of a superposition of spherical functions:

$$v_i^p = \sum_{l,m} a_{p\,l\,m}\,\frac{1}{r}\, j_l(z\xi)\; Y_l^m(\theta,\, \phi)\exp(-\mathrm{i}\omega t) , \tag{2}$$

where $z \equiv n\,x$, $\xi \equiv r/a$, $j_l(z) \equiv \sqrt{\pi\, z/2}\, J_{l+1/2}(z)$ is the Riccati–Bessel function, $J_{l+1/2}(z)$ is the Bessel function, and $Y_l^m(\theta,\, \phi)$ is the spherical function. For $r > a$, the field consists of the field of a wave incident on the ball:

$$v_0^p(\mathbf{r},\, t) = v_0^p \exp\left[\mathrm{i}\,(\mathbf{kr} - \omega t)\right]$$

and the scattered radiation field

$$v_{\mathrm{s}}^p = \sum_{l,m} b_{p\,l\,m}\,\frac{1}{r}\, h_l(x\xi)\; Y_l^m(\theta,\, \phi)\, \exp(-\mathrm{i}\,\omega t) , \tag{3}$$

where $h_l(z) \equiv \sqrt{\pi\, z/2}\, H^{(1)}_{l+1/2}(z) = j_l(z) + \mathrm{i} y_l(z)$, and $H^{(1)}_{l+1/2}(z)$ is a Hankel function of the first kind. If the time dependence of the electromagnetic field is taken in the form $\exp(\mathrm{i}\omega t)$, then a Hankel function of the second kind, $H^{(2)}_{l+1/2}$, enters into the formulas instead of $H^{(1)}_{l+1/2}$ [26, 48]. Coefficients a_{plm} and b_{plm} in Eqns (2), (3) are found from the continuity conditions for the tangential components of vectors **E** and **H** at the ball surface. Coefficients a_{plm} and b_{plm} being determined, the electromagnetic field can be calculated at any point in space.

The extinction cross section σ_{ext} is used as an integral characteristic of scattering. It is introduced as the ratio of the absorbed and scattered radiation power to the electromagnetic wave energy flux [32, 46]. (If light absorption inside the ball is absent, σ_{ext} coincides with the light scattering cross section.) The ratio of σ_{ext} to the cross section πa^2 of the ball is denoted by Q_{ext}. According to the Lorenz–Mie theory, the normalized extinction cross section is given by

$$Q_{\mathrm{ext}} = \frac{2}{x^2}\sum_{p=0}^{1}\sum_{l=1}^{\infty}(2l+1)\,\mathrm{Re}\,\alpha_{pl} . \tag{4}$$

Here, the following notation was used:

$$\alpha_{pl} = \frac{n^{1-2p}\, j_l'(z)\, j_l(x) - j_l(z)\, j_l'(x)}{D_{pl}(x,\, n)} , \tag{5}$$

where

$$D_{pl}(x,\, n) \equiv n^{1-2p}\, j_l'(z)\, h_l(x) - j_l(z)\, h_l'(x)$$

(the prime labels the derivative of the function with respect to its argument). Formula (4) is usually called the Mie expansion, and the coefficients α_{pl} are known as the Mie scattering functions.

In order to estimate the coefficients of expansion in formula (4), expression (5) can be rewritten as

$$\alpha_{pl} = \frac{1}{1 + \mathrm{i}\, u_{pl}} , \tag{6}$$

where

$$u_{pl} = \frac{n^{1-2p}\, j_l'(z)\, y_l(x) - j_l(z)\, y_l'(x)}{n^{1-2p}\, j_l'(z)\, j_l(x) - j_l(z)\, j_l'(x)} .$$

For the real parameter n, the expression u_{pl} conforms to a real quantity. Therefore, the real part of coefficient (6):

$$\mathrm{Re}\,\alpha_{pl} = \frac{1}{1 + u_{pl}^2}$$

changes from 0 to 1. Instead of the real function u_{pl}, the phase angle δ_{pl} is often introduced in the following way

$$u_{pl} = \cot\delta_{pl} .$$

In this case, the expression for the extinction cross section assumes the form

$$Q_{\mathrm{ext}} = \frac{2}{x^2}\sum_{p=0}^{1}\sum_{l=1}^{\infty}(2l+1)\,\sin^2\,\delta_{pl} .$$

By way of illustration, Fig. 1 shows the function $Q_{\mathrm{ext}}(x)$ calculated for a ball with $n = 1.5$. The curve in Fig. 1b passes

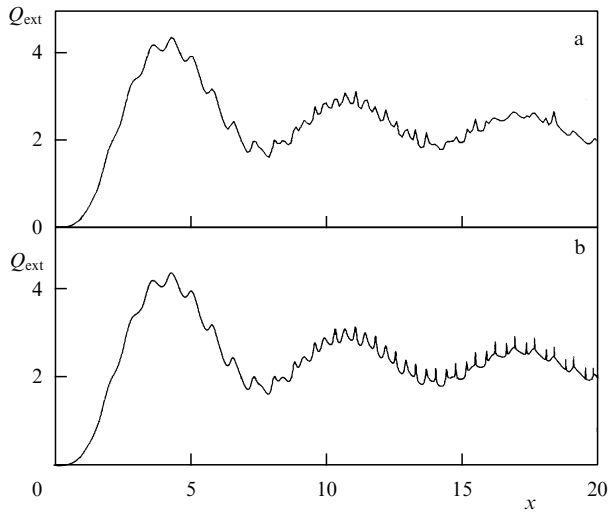

Figure 1. Normalized scattering cross section for a dielectric ball with refractive index $n = 1.5$ versus the parameter x.

actually through a set of points $(x, Q_{ext}(x))$ spaced at $\Delta x = 0.005$. The curve in Fig. 1a shows the same calculated dependence borrowed from book [32, Fig. 32]. This curve can be obtained if $Q_{ext}(x)$ is computed assuming $\Delta x = 0.1$. The hyperfine structure of the Mie scattering cross section [49] in the range $x = 15-20$ (see Fig. 1b) is inapparent in Fig. 1a. This obvious distinction between the two curves indicates that the calculation of $Q_{ext}(x)$ has until recently presented a complicated computational problem. The difficulty of computation stimulated the search for an analytical solution to the scattering problem as an alternative to the Mie expansion (see, for instance, Refs [50, 51]). However, the algorithm of calculation of coefficients α_{pl} proposed in paper [18] combined with modern computing techniques simplify the task.

The dependence $Q_{ext}(x)$ at large x is characterized by sets of equidistant peaks [52–59]. Specifically, two peak clusters in Fig. 1b for $x = 15-20$ correspond to the excitation of TE and TM polarization modes. The quantity x for a resonance mode with a number l lies in the vicinity of

$$x_l \simeq \frac{1}{n}\left(l + \frac{1}{2}\right)$$

(the mode number is sometimes called the angular momentum index). Therefore, the distance between identically polarized modes is equal to $\Delta x = 1/n$ [56]. At the resonance frequency, the imaginary part of the denominator in the right-hand side of formula (5) becomes zero, $u_{pl} = 0$, and $\mathrm{Re}\,\alpha_{pl} = 1$ [26, 52].

3. Enhanced probabilities of spontaneous emission

One of the interesting characteristics of optical microresonators is a change in the Einstein coefficients for spontaneous emission. This was first noticed in work [60]. If the radiative transition with a dipole moment μ_d is possible between the energy levels of a particle, then it follows from Ref. [60] that the probability (s^{-1}) of spontaneous emission equals

$$A = \frac{8\pi v^2}{c^3}\, hv\, \frac{8\pi^3 \mu_d^2}{3h^2},$$

where $8\pi v^2/c^3$ is the spectral photon density in a vacuum. However, for a system in the resonant cavity, the factor $8\pi v^2/c^3$ no longer gives the right number of oscillations per unit volume and unit frequency. Now there is a single cavity-related oscillation over the frequency range v/Q, and hence the probability of spontaneous emission increases by the quantity

$$f = \frac{3\,Q\,\lambda^3}{4\,\pi^2\,V}, \tag{7}$$

where V is the resonator volume.

In the language of qualitative estimates, droplets may be said to have extremely high Q values at small volumes V [36, 37]. Therefore, the Einstein coefficient A may increase by a few orders of magnitude. A strict theoretical proof of this idea is provided in papers [61–63]. The relevant experimental data can be found in works [64, 65] (see also the review [66]).

Ching et al. [61] reported on the resonant properties of the electromagnetic field in a dielectric ball with real n, placed inside a hollow conducting sphere of radius Λ, as $\Lambda \to \infty$. An infinitely remote surface at which the tangential component of $\mathbf{E}$ vanishes was introduced into the model for the correct quantization of the electromagnetic field, taking into account the energy dissipation from the resonator. This may be regarded as a standard approach to the study of media inhomogeneous in one direction [67–69]. Vectors $\mathbf{E}(\mathbf{r}, t)$ and $\mathbf{H}(\mathbf{r}, t)$ were found by their expansion in terms of the real electric $\mathbf{e}(s, \mathbf{r})$ and magnetic $\mathbf{b}(s, \mathbf{r})$ eigenfunctions [61]:

$$\mathbf{E} = \sum_s \omega_s^{-1}\, \frac{\mathrm{d}\,\alpha(s,t)}{\mathrm{d}t}\, \mathbf{e}(s,\mathbf{r}), \tag{8}$$

$$\mathbf{H} = \sum_s \alpha(s,t)\, \mathbf{b}(s,\mathbf{r}), \tag{9}$$

$$\nabla \times \mathbf{e}(s,\mathbf{r}) = -\frac{\omega_s}{c}\, \mathbf{b}(s,\mathbf{r}).$$

Here, the constants ω_s are frequencies. The eigenvector $\mathbf{e}(s, \mathbf{r})$ presents the solution of the equation

$$\nabla \times \left[\nabla \times \mathbf{e}(s,\mathbf{r})\right] = \frac{\omega_s^2}{c^2}\, \varepsilon(\mathbf{r})\, \mathbf{e}(s,\mathbf{r}),$$

where $\varepsilon(\mathbf{r}) = n^2$ at $r \leqslant a$, and $\varepsilon(\mathbf{r}) = 1$ at $r > a$. The coefficients $\alpha(s, t)$ of expansion satisfy the equations

$$\frac{\mathrm{d}^2\,\alpha(s,t)}{\mathrm{d}t^2} = -\omega_s^2\,\alpha(s,t).$$

The normalization of $\mathbf{e}$ and $\mathbf{b}$ was chosen in such a way that the relations

$$I^{(1)}(s,s') = I^{(2)}(s,s') = \hbar\omega_s\,\delta_{ss'} \tag{10}$$

be fulfilled, where

$$I^{(1)}(s,s') = \frac{1}{4\pi}\iiint_{r<\Lambda} \varepsilon(\mathbf{r})\,\mathbf{e}(s,\mathbf{r})\,\mathbf{e}(s',\mathbf{r})\,\mathrm{d}V,$$

$$I^{(2)}(s,s') = \frac{1}{4\pi}\iiint_{r<\Lambda} \mathbf{b}(s,\mathbf{r})\,\mathbf{b}(s',\mathbf{r})\,\mathrm{d}V.$$

Expansions (8) and (9) are used to write the total energy of the electromagnetic field as

$$\frac{1}{8\pi}\iiint(\varepsilon\,\mathbf{E}\,\mathbf{E}+\mathbf{H}\,\mathbf{H})\,\mathrm{d}V=\sum_s N_s\iiint u_s(\mathbf{r})\,\mathrm{d}V.$$

The integral of motion in the right-hand part of this expression:

$$N_s=\frac{1}{2}\left\{\frac{1}{\omega_s^2}\left[\frac{\mathrm{d}\,\alpha(s,t)}{\mathrm{d}t}\right]^2+\alpha^2(s,t)\right\}$$

is the number of quanta in mode s, and

$$u_s(\mathbf{r})=\frac{1}{8\pi}\left[\varepsilon(\mathbf{r})\,\mathbf{e}(s,\mathbf{r})\,\mathbf{e}(s,\mathbf{r})+\mathbf{b}(s,\mathbf{r})\,\mathbf{b}(s,\mathbf{r})\right]$$

is the energy density of the electromagnetic field in which there is one quantum per mode s. According to relations (10), the function $u_s(\mathbf{r})$ is normalized to $\hbar\omega_s$, so that $(1/\hbar\omega_s)\,u_s(\mathbf{r})$ is the probability of finding a photon in mode s at point $\mathbf{r}$ in space. Thus, the local density of states of the electromagnetic field falling within the unit frequency range about ω is given by

$$\rho(\omega,\,\mathbf{r})=\frac{1}{\hbar\omega}\sum_s\delta(\omega-\omega_s)\,u_s(\mathbf{r})\,. \tag{11}$$

In the right-hand side of formula (11), summation is over the indices p, l, m introduced earlier and also over the radial quantum number v of the system consisting of the ball and conducting sphere. In the $\Lambda\to\infty$ limit, the distance between radial modes tends to zero, which makes it possible to pass from the summation over v to integration:

$$\sum_v\to\frac{\Lambda}{\pi c}\int\mathrm{d}\omega_s\,.$$

After integration of expression (11) over the frequency ω_s and the angles θ, ϕ and summation over m, Ching et al. [61] undertook a detailed analysis of the following ratios

$$g(x,\,n;\,\xi)\equiv\frac{\rho(\omega,r)}{\rho_{\mathrm{v}}(\omega)},\quad G(x,n)\equiv\frac{\rho^{\mathrm{C}}(\omega)}{\rho_{\mathrm{v}}(\omega)\,V}\,,$$

where

$$\rho^{\mathrm{C}}(\omega)\equiv\int_0^a\rho(\omega,r)\,r^2\,\mathrm{d}r\,, \tag{12}$$

$$V\equiv\frac{4\pi}{3}\,a^3\,,\quad\rho_{\mathrm{v}}(\omega)=\frac{\omega^2}{\pi^2\,c^3}\,,\quad\xi\equiv\frac{r}{a}\,.$$

The quantity g characterizes the alteration of the local density of states at a distance r from the center of the ball as compared with a vacuum of infinite extent. The quantity G is the ratio of the spectral density of states of the electromagnetic field in the whole ball to the spectral density of states in the infinite vacuum volume V. The graphs of $g(x)$, $g(\xi)$ and $G(x)$ published in paper [61] correspond to the dependences

$$g(x,n;\xi)=\frac{n}{4\,x^2\,\xi^2}\sum_{p=0}^{1}\sum_{l=l}^{\infty}(2l+1)\left|\frac{n^{1-2p}\,j_l(z\xi)}{D_{pl}(x,n)}\right|^2\times\left[1+\frac{l\,(l+1)}{z^2\,\xi^2}+\left(\frac{j_l'(z\xi)}{j_l(z\xi)}\right)^2\right], \tag{13}$$

$$G(x,n)=\frac{3\,n}{x^2}\sum_{p=0}^{1}\sum_{l=1}^{\infty}(2l+1)\left|\frac{n^{1-2p}\,j_l(z)}{D_{pl}(x,n)}\right|^2\times\left[1-\frac{l\,(l+1)}{z^2}+\left(\frac{j_l'(z)}{j_l(z)}\right)^2\right]. \tag{14}$$

Of importance in functions $g(x,n;\,\xi)$ (13) and $G(x,n)$ (14) is the factor $|D_{pl}(x,n)|^{-2}$ analogous to the factor $D_{\bar{p}\bar{l}}^{-1}(x,n)$ in the formula for the Mie expansion coefficient (5).

With the condition $\mathrm{Im}\,D_{pl}(x,n)=0$ being fulfilled and the quality factor of the corresponding WGM being sufficiently high, a sharp resonance peak emerges in the dependence of ρ^{C} on x [just as in the dependence $Q_{\mathrm{ext}}(x)$]. Ching et al. [61] stated basic principles for the prediction of the resonance position and amplitude in $\rho^{\mathrm{C}}(\omega)$. To illustrate the peculiarities of the density of states (12), Fig. 2 compares the functions $G(x,1.4)$ and $Q_{\mathrm{ext}}(x,1.4)$. It can be seen that the narrow resonance peaks in functions $G(x,1.4)$ and $Q_{\mathrm{ext}}(x,1.4)$ occur at the same frequencies. Nevertheless, if the quantity Q_{ext} at a resonance frequency is comparable with Q_{ext} at nonresonance frequencies, the amplitude of $G(x,n)$ maxima lies in the range of 40–90.

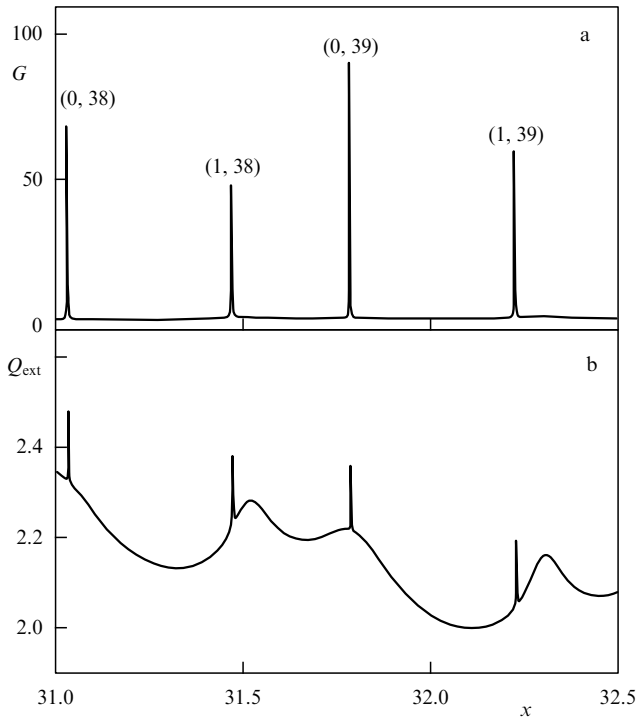

Figure 2. Normalized density of states G (a) and the extinction cross section Q_{ext} (b) versus parameter x for a dielectric microball with $n=1.4$. The peaks are labeled by indices $(p,\,l)$.

That the maxima in $G(x,n)$ actually exist by virtue of surface WGM is shown by the following figures. Figure 3 presents the quantity g as a function of the position ξ inside the droplet. The $g(\xi)$ dependence allows a contribution to $G(x,n)$ from different parts of the droplet to be estimated because the following relationship takes place

$$G(x,n)=3\int_0^1 g(x,n;\xi)\,\xi^2\,\mathrm{d}\xi\,.$$

It follows from Fig. 3a that the main contribution to $G(x,n) \simeq 90$ at a resonance frequency $\omega_{0,39}$ comes from a narrow area near the droplet surface, where $g \simeq 300$. At a nonresonance frequency, however, $g(x,n;\xi) \leqslant 3$ (see Fig. 3b).

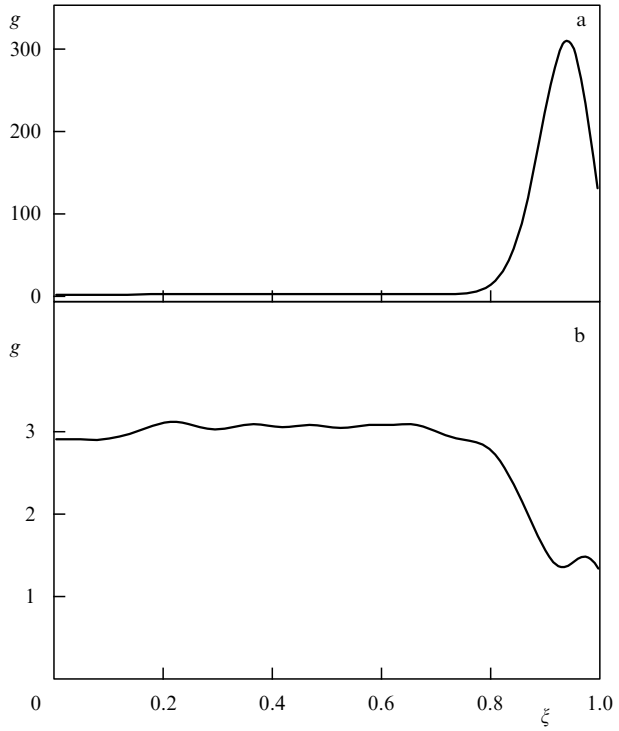

Figure 3. Normalized local density of states g versus parameter ξ for $n = 1.4$ and $x = 31.7892$ (which corresponds to a resonance peak with $p = 0$ and $l = 39$) (a) and $x = 31.9000$ (b).

It should be noted that the parameters G and g are of the same order of magnitude as factor (7). They can be used for the qualitative description of the change in the probability A^{C} of spontaneous radiation in the droplet compared with the probability A_{v} of spontaneous radiation in a vacuum. The factor G characterizes the ratio of the Einstein coefficients $\langle A^{\mathrm{C}}/A_{\mathrm{v}}\rangle$ averaged over the whole droplet volume, while the factor g characterizes the ratio $A^{\mathrm{C}}/A_{\mathrm{v}}$ averaged over angles θ and ϕ but not over the distance from the droplet center r. The validity range of the model predicting a rise in $A^{\mathrm{C}}/A_{\mathrm{v}}$ at resonance frequencies was outlined in paper [62].

The conclusions drawn in papers [61, 62] are consistent with the results of other studies. Chew [70, 71] reported the derivation, in the framework of classical electrodynamics, of formulas for the dipole radiation powers $R^{\perp}/R_0^{\perp}$ and $R^{\parallel}/R_0^{\parallel}$ of an atom located inside or outside a dielectric ball. Superscripts $\perp$ and $\parallel$ indicate dipole oscillations normal and parallel to the ball surface, respectively, and R_0 is the radiation power in the absence of the ball. The formulas for the ratio of radiation powers [as well as formulas (14) and (13)] contain factors $|D_{pl}(x,n)|^{-2}$. For this reason, as shown in works [70, 71], the radiation power in droplets may increase hundreds of times. This is possible if the dipole oscillation frequency coincides with the WGM resonance frequency of the dielectric ball, while the dipole itself is positioned close to its surface. The calculation of the power ratio $\langle R/R_0\rangle$ averaged over the dipole orientation and location in the droplet yields the same result as the calculation of $\langle A^{\mathrm{C}}/A_{\mathrm{v}}\rangle$.

The theory of inelastic light scattering (Raman scattering and fluorescence) in a dielectric ball has been developed by Chew et al. [72–75]. This theoretical model also makes use of classical electrodynamics. Specifically, the molecules re-emitting light are regarded as oscillating dipoles induced by the incoming electric field and inserted in the ball. It has been shown that the dipole radiation strongly depends on its location inside a spherical particle and resonant optical properties of the ball.

Changes in radiation characteristics of a droplet-forming liquid can be illustrated by the following schematic diagram [76]. Figure 4 compares the fluorescence spectra from the dye-containing liquid and the same liquid in the form of a droplet. For the droplet, the fluorescence efficiency at certain discrete emission wavelengths is enhanced, whereas the fluorescence efficiency at other wavelengths is inhibited. The resonance position in the spectrum is strongly dependent on the droplet structure (for instance, its size, refractive index). Hence the term morphology-dependent resonances [77–84]. The amplitude of each resonance is proportional to the resonator quality factor, while its width is inversely proportional to Q-factor [83, 85]. Therefore, the fluorescence efficiencies of an optical cell and a droplet, integrated over a broad spectral range, would be roughly equal.

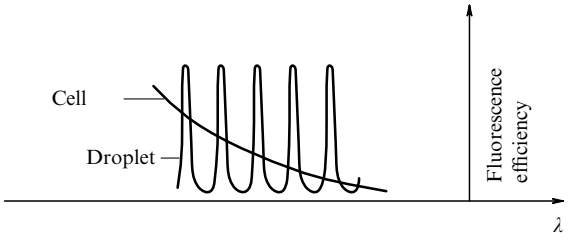

Figure 4. Typical spectral profiles of fluorescence efficiency for an optical cell and a droplet [76].

Figure 4 gives a schematic illustration of the enhancement and suppression of fluorescence efficiency. The real fluorescence spectrum of a dye-containing polymeric microball is shown in Fig. 5. Structural resonances in the fluorescence spectrum have the same origin as the sharp peaks in the Mie light scattering spectra. These resonances result from WGM excitation [49, 52].

Because the droplet is considered to be an optical resonator, it is important to evaluate its quality factor which characterizes energy dissipation from the resonator and is defined by the following formula [47]

$$\frac{1}{Q} \equiv \frac{1}{\omega \langle W(t)\rangle} \left\langle \frac{\mathrm{d}}{\mathrm{d}t} W(t) \right\rangle = \frac{2\omega''}{\omega'} .$$

Here, $W(t)$ is the energy of the electromagnetic mode, $\omega = \omega' + \mathrm{i}\omega''$ is the angular frequency, and the angular brackets $\langle \ldots \rangle$ denote averaging over the oscillation period $T = 2\pi/\omega'$.

A characteristic equation for the mode frequency ensues from the continuity conditions for the tangential components of **E** and **H** at the ball surface [47]:

$$D_{pl}(x,n) = 0 . \qquad (15)$$

By appearance, this equation coincides with the condition of zero denominator in the right-hand side of expressions (5),

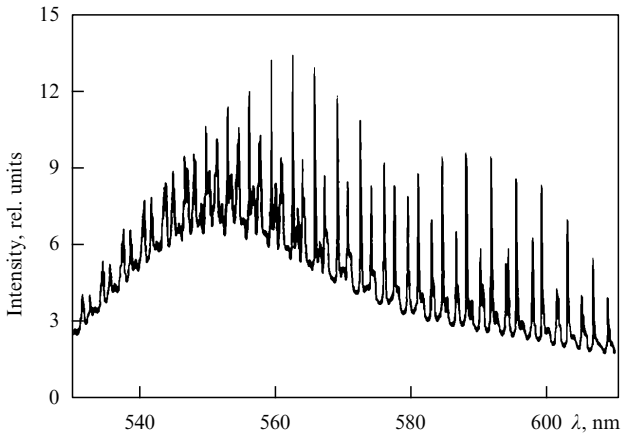

Figure 5. Rhodamine 6G fluorescence spectrum in a polymeric particle [86].

(13), (14). It should be borne in mind, however, that the parameter x in formulas (5), (13), (14) is a real quantity, whereas it is a complex one in Eqn (15). The characteristic equation (15) may be used to determine both the frequency of resonance mode (ω') and its imaginary part (ω''). Indeed, the employment of asymptotic expressions for the Bessel and Hankel functions yield the following formula for ω [47, 53–58]:

$$\omega = \frac{c}{na}\left[l + \frac{1}{2} - (t_q + \Delta t)\beta\right]. \tag{16}$$

Here, t_q is the qth root of the equation

$$\mathrm{Ai}(t_q) = 0\,, \quad q = 1, 2, 3, \ldots, \quad t_q < 0\,,$$

where Ai is the Airy function, and the number q is called the mode order or radial mode index, and in addition

$$\Delta t = n^{1-2p}\,\frac{1 + \mathrm{i}\exp(-2T)}{\beta\sqrt{n^2-1}}\,,$$

$$T \equiv \left(l + \frac{1}{2}\right)(\eta - \tanh\eta)\,, \quad \left(\frac{3T}{2}\right)^{2/3} \gg 1\,,$$

$$\cosh\eta = n\left[1 - \frac{1}{l + 1/2}\left(t_q\beta + \frac{n^{1-2p}}{\sqrt{n^2-1}}\right)\right]^{-1}.$$

The formalism developed in monograph [47] allows the main properties of WGM to be predicted. The modes are degenerate in azimuthal mode number m which acquires $2l + 1$ values ($-l \leqslant m \leqslant l$). The width of the layer of WGM energy localization in the radial direction is determined by the quantum number q and equals $|t_q|\,\beta\lambda/2\pi n$ [53]. (The effective mode volume was computed in Refs [37, 44, 53].) At $x \leqslant 30$, the excitation of modes with $q > 1$ may be neglected (all resonance peaks in Fig. 2 correspond to $q = 1$).

The theory of open resonators [47] yields an abnormally high emission Q-factor of microdroplets. For example, it must be of the order of 10^{73} at $\lambda = 0.6$ μm for a drop of water with radius 50 μm. This Q value is much greater than typical values of $Q \simeq 10^7 - 10^8$ obtained in experiment [76, 85, 87].

The deviation of a droplet surface from the ideal spherical shape must be taken into account for the correct calculation of a Q-factor [37, 56, 88–90].

A theoretical study in the framework of quantum electrodynamics has demonstrated that surface perturbations remove the azimuthal degeneracy of modes in a multiplet [39, 88–90]. The predicted effect is corroborated by the results of measuring emission spectra from flowing deformed droplets with high temporal and frequency resolution. Experimental studies have been designed to observe spectra of stimulated Raman scattering (SRS) [91, 92], fluorescence [93], and laser radiation [94]. A shift $\Delta\omega$ of the mode frequency relative to the initial value of ω was computed for minor shape distortions, when the droplet surface could be approximated by an ellipsoid. For an ellipsoid showing a small deviation from an ideal sphere, the frequency shift of each WGM is given by the following formula [88]

$$\frac{\Delta\omega_m}{\omega} = \frac{\epsilon}{6}\left[\frac{3m^2}{l(l+1)} - 1\right],$$

where $\epsilon = (r_{\mathrm{pol}} - r_{\mathrm{eq}})/a$, r_{pol}, r_{eq} are the polar and equatorial radii, respectively, while the small parameter ϵ is positive for a prolate ellipsoid, and negative for an oblate one. The frequency shift is independent of the polarization (TE or TM), radial mode order q, and droplet radius a.

The theory suggested that the multiplet splitting may be followed by impaired WGM quality factor. The assumption that radiation involves all members of the multiplet in a coherent fashion has led to a theoretical estimate of Q-factor consistent with experimental findings. However, the theory failed to predict the broadening of individual multiplet components, the widths of which showed but a weak dependence on $\Delta\omega_m$. In other words, according to Lai et al. [88, 89], the emission Q-factor of a deformed droplet must not decrease upon the excitation of a solitary mode regardless of the remaining modes of the multiplet.

A simpler model [56] used the theory of diffraction of electromagnetic waves. A formula for the radiation quality factor was proposed, which took into account light scattering from inhomogeneities at the resonator surface. It was found that thermal capillary vibrations of the droplet surface with amplitudes of the order of 3×10^{-4} μm reduced Q-factor to the values observed in experiment.

The higher the Q values, the narrower the structural resonances in the droplet radiation spectra, since the resonance width $\Delta\lambda = \lambda/Q$ [83,85]. Hence, the measurement of peak positions in emission spectra may be used to accurately describe the droplet structure.

4. Structural analysis of droplets

Mie scattering spectra have been used to identify droplets since the 1960s [95–97]. Two approaches have been developed based on the Lorenz–Mie theory. The early method measures scattered light intensity as a function of scattering angle (frequently referred to as the phase function). The other approach, the so-called optical resonance technique, is based on the measurements of light intensity at fixed angles and varying x. The two methods were compared by Ray et al. [97]. In this experiment, both mono- and multicomponent aerosols were studied. In slowly evaporating droplets of radius 10 μm, the changes of the order of 1 Å were measured for the droplet radius. The use of the optical resonance technique ensured that the error in measuring the macroscopic parameter was smaller than the molecular size. The relative measurement

error was greater for multicomponent aerosols and rapidly evaporating droplets, amounting to 10^{-4} in both droplet radius and refractive index measurements.

Devarakonda et al. [98] described a method for droplet diagnosis based on the analysis of resonance positions in elastic and Raman light scattering spectra. The method was applied to studying rapid evaporation of a linear stream of monodispersed ethanol droplets. The droplet radius was $a \simeq 10$ μm, and the distance between neighboring droplets amounted to 40 μm. The experimental facility was used to simultaneously measure changes of the droplet radius (Δa) and refractive index in the fluid [98]. The latter parameter varied as evaporating droplets cooled. The fluid temperature was determined to an accuracy of 0.25 °C.

The ratio of a measurement error Δa to a was approximately 10^{-4}. In principle, the measurements could be made at 10 μs intervals. The experiment was designed in such a way that the ethanol content in the gas surrounding the droplets might be neglected. This condition satisfied, the measured droplet evaporation rate in a stream turned out to be thrice lower than the predicted evaporation rate of an individual droplet. This difference was attributed to interactions between droplets in the course of evaporation. The observed effect of interdroplet interaction was first described in paper [99].

A scheme for the computation of the size distribution function of scattering particles based on experimental data on multiple scattering of electromagnetic radiation has been developed in a series of theoretical works [100 – 103]. Weber and Schweiger [104] described a state-of-the-art experimental setup for the diagnosis of aerosols by photon correlation spectroscopy. This apparatus enables researchers to simultaneously measure the local size, concentration, and velocity of travel of submicron particles.

According to Holt and Crum [105], a Mie scattering diagram may also be used in experimental studies of spherical cavities in a fluid. This means that the precise optical diagnostics is applicable to cavitation studies too [106 – 108].

A diagnostic technique based on the measurement of droplet fluorescence spectra has been proposed by Benner et al. [79]. Their paper gave incentive to a series of experiments with fluorescent dye added to droplets [80, 109 – 112]. Rhodamine at a relative concentration of 10^{-4} was most frequently used for the purpose. In early experiments, the growth and evaporation rates of ethanol droplets with radius 30 μm were determined [109]. A simple relationship

$$\frac{\Delta a}{a} = \frac{\Delta \lambda}{\lambda}, \tag{17}$$

was employed in measurements, which describes the dependence of the structural resonance wavelength on the radius a. Equality (17) is applicable provided the droplet's temperature and chemical composition remain unaltered.

The use of relationship (17) in experiment [109] allowed changes Δa within 0.7 nm to be determined for a linear stream of monodispersed droplets. The droplet evaporation rate was found to equal 25 μm s^{-1}. The relative measurement error was estimated as

$$\frac{\Delta a}{a} = 2 \times 10^{-5}.$$

Further improvement of the fluorescence technique facilitated the observation of more complicated effects. In Ref. [113], the time dependences of spectral characteristics were used to study damped oscillations of ethanol droplets with $a = 20$ μm. Surface oscillations were induced by droplet irradiation with laser pulses having an energy of 0.15 μJ. Oscillation amplitude amounted to $5 \times 10^{-4} a$. The fluorescence spectra obtained in the study allowed the determination of the surface tension and ethanol fluid viscosity for separate droplets.

5. Lasing in droplets

In fluorescence studies of dye-containing droplets, the pump radiation intensity varied over a broad range. It was found that a rise in pumping intensity led to a nonlinear increase of radiation efficiency at definite WGM frequencies and concurrent narrowing of radiation lines [114, 115]. A typical pattern of the emission process nonlinear in the pump radiation intensity is depicted in Fig. 6. The figure shows that the effect of stimulated emission is superimposed on that of the enhanced Einstein coefficient A [14]. When stimulated emission prevails over spontaneous, the optical process is referred to as lasing. In other words, under certain conditions, a droplet can be regarded as a whispering-gallery-mode laser [87].

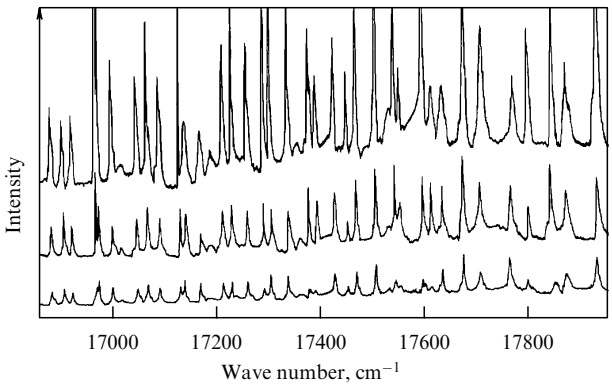

Figure 6. Three typical emission spectra of rhodamine contained in 14-μm diameter ethanol droplets pumped by an Ar^+ laser at 514.5 nm [115]. The laser pump intensity was increased by a factor of 1.5 for each new spectrum.

The lasing threshold in a droplet was first observed by Tzeng et al. [114]. In this experiment, the individual ethanol droplets around 60 μm in diameter were subjected to continuous radiation from an Ar^+ laser at $\lambda = 514.5$ μm. The incident laser intensity P was focused onto a 200-μm spot and gradually increased from 10^{-4} to 1 W. It turned out that the lasing threshold was reached at $P = 10^{-2}$ W. It may be concluded that nonlinear optical processes can be observed at low pump intensities due to the small droplet size and high Q values.

6. Stimulated Raman light scattering

Lasing is not the sole nonlinear optical process observed in experiment. A large number of publications concern Raman scattering (RS) of light in droplets. Studies along this line were initiated in the late 1960s in response to the advance of cell biology and investigations into atmospheric aerosols. References to the early works can be found in paper [72]. The pioneering studies reported by Bykovskiĭ et al. [116, 117]

resulted in the discovery of RS from shape oscillations of liquid spherical particles.

In one of the first works, Raman spectroscopy was used to study microparticle behavior on a substrate [118]. Ten years later optical levitation of microparticles was proposed [119–122], i.e. a method for optical fixation of particles with the aid of a light field. First, a RS spectrum from isolated glass microbeads was recorded [119, 120]. Thereafter, Raman spectra of optically levitated droplets of water:glycerol mixtures were investigated [121]. In Ref. [122], spontaneous Raman scattering spectra from droplets of dioctyl phthalate, a phthalic acid ether, were compared with the corresponding spectra from bulk samples.

Another technique consists in electrodynamic suspension of droplets [123–127], which may require the computation of shape oscillations of the charged liquid sphere. This problem was first considered by Rayleigh [128]. Its present-day solution has been offered by Feng and Beard [129].

The investigation of droplet streams in addition to that of separate suspended droplets has been extensively carried out since 1984 [130–136].

Taking into account the known features of RS in droplets, the following areas of research can be distinguished as most promising: comparison of resonance structure in elastic and Raman light scattering spectra [72, 75, 98, 137–140]; competition between lasing and RS [141] including suppression of the former by stimulated RS [142]; SRS investigation [91, 130, 136, 143–151] including the observation of coherent anti-Stokes RS [134, 52], stimulated anti-Stokes RS, and stimulated resonant RS [154]; high-order SRS [134, 155–157]; stimulated Brillouin scattering [149, 157–160], and third harmonic generation in droplets [161, 162].

In experimental studies [127, 163], SRS from optical cells was compared with light oscillations at the Stokes frequency in microdroplets. Naturally, the mechanisms of Raman light scattering in both systems were identical. The difference was reduced to a much higher efficiency of nonlinear processes in the droplets [150]. In a qualitative interpretation, a droplet was considered to be a lens enhancing incident radiation intensity and a resonator providing optical feedback [164]. By virtue of the above features, the number of Stokes lines in the RS spectrum from a droplet is significantly higher than in the case of light scattering from an ordinary fluid. That is, only first-order Stokes lines are usually observable in optical cells. It is argued by Qian et al. [163] that the authors of a droplet experiment [165] observed Stokes radiation of up to the seventeenth order. A detailed kinetic description of the sequential excitation of high-order Stokes radiation can be found in Refs [155–157].

The high efficiency of Raman scattering in droplets was used as a tool for the development of relevant diagnostic techniques. Carls et al. [166] evaluated the possibility of employing time-resolved Raman spectroscopy for studying chemical reactions in aerosol microdroplets. As a test reaction, the absorption of D_2O vapor by optically levitated glycerol droplets was examined. By comparing the relative amplitudes of various RS spectral components, the composition of the suspended droplets was estimated as a function of time. Specifically, the number ratio of ^-OD bonds in D_2O molecules to ^-CH bonds in glycerol system was deduced. In addition, the average temperature of optically levitated droplets in this system is liable to measure.

Acker et al. [167] employed SRS phenomenon for diagnostics of fuel spraying in diesel engines. The authors demonstrated the possibility of determining both the size and the chemical composition of the droplets produced as the fuel blends were sprayed. In order to better illustrate the applicability of diagnostic methods with which to analyze combustion processes, color photography was used to portray aerosols and obtain photographs of the fuel sprays with the aid of green and red optical filters. (The illumination source for a stream of droplets was the second harmonic output of a neodymium laser with $\lambda = 532$ nm and a pump intensity of around 1 GW cm^{-2}.) It was shown that various constituents of the aerosol such as liquid sheets and ligaments, large and small microdroplets, and fuel vapors contributed to the green light produced by elastic scattering of incident radiation [76]. At the same time, only large microdroplets with $a > 20$ μm gave rise to red scattered radiation due to SRS effect in droplets with a sufficiently high quality factor.

Figure 7 shows SRS spectra from individual microdroplets ($a \simeq 45$ μm) of various fuels, measured in a monodispersed stream produced by a Berglund–Liu generator based on a fluid spraying away through the vibrating orifice. The SRS spectra clearly demonstrate the presence of a cyclic mode of the toluene carbon ring with a frequency around 1000 cm^{-1} and the modes of pentane stretching vibrations with frequencies close to 2900 cm^{-1}. It may be concluded that the analysis of intensities of stimulated Raman scattering with different frequency shifts may be used to determine the relative concentrations of toluene and pentane in droplets.

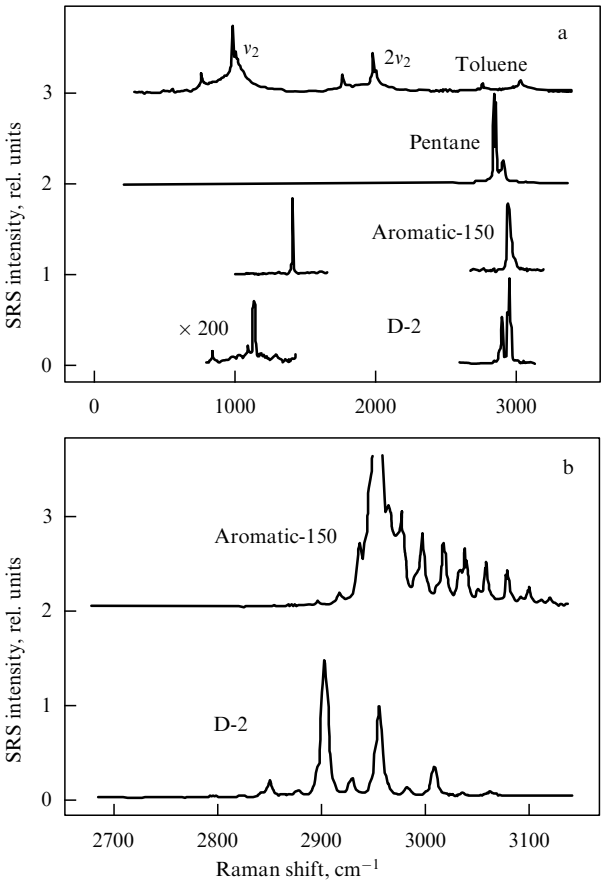

Figure 7. Multishot averaged SRS spectra from droplets of various fuels: toluene, pentane, Exxon Aromatic-150, and Mobil D-2 [167]. The vertical axis shows the first-order Stokes radiation intensity, the horizontal the Raman shift from the frequency of incident laser radiation.

By using optical methods to study combustion, it is also possible to measure flame temperature. For example, paper [168] describes an installation diagram for measuring the local temperature distribution near a stream of droplets from the parameters of coherent anti-Stokes scattering of light in the flame of burning methanol droplets.

In Refs [123 – 127], Raman scattering of light was used for examining the droplets of aqueous solutions of inorganic salts, such as sulfates and nitrates. Examination with a high-resolution monochromator revealed fine-structure spectral responses suggesting phase transitions in droplets of supersaturated fluids and the influence of cations on the anions' Raman spectra. This approach is interesting in that it allowed one to avoid the effects of the container's walls and impurities on the phase transition kinetics and thus achieve an extremely high degree of supersaturation in the solution droplets. Due to this, the interaction between the cations and anions gave rise to new spectral lines of radiating molecules, which had not been observed earlier either in volumetric solutions or bulk crystalline samples [127]. The crystal phase produced in a droplet differed from the phase that came to form in bulky solution [169, 170].

Vehring et al. [170] described a method for the analysis of the chemical composition of air-borne particles from RS spectra. The experimental setup allowed impurities with a mass of nearly 10^{-10} g to be detected in a microparticle from 1 to 10 μm in diameter. With an impurity content in excess of 10 pg, the authors of Ref. [170] were able not only to identify molecular lines but measure intermolecular interaction forces as well. Specifically, they managed to determine the type of crystalline phase arising in microparticles of a supersaturated sodium sulfate aqueous solution.

Schweiger [171] did a review of experimental studies reporting the use of RS for microparticle diagnostics, which were published before 1990. The review can be added by references to more recent experiments with inorganic [139, 169, 172 – 175] and organic [176 – 188] microparticles and to investigations into chemical processes in suspended droplets [189 – 195].

The so-called input and output resonances make a characteristic feature of fluorescence and RS spectra in droplets [65, 80, 139, 140, 178, 184, 196 – 198]. It is especially well apparent in the measurement of the time dependence of RS spectra from isolated droplets undergoing evaporation. Output resonances occur if condition (16) for the scattered light frequency is satisfied. Evaporation causes a decrease of the droplet diameter and a shift of structural resonance in the RS spectrum towards its shorter wavelength edge. At a constant evaporation rate, the time dependence of the scattered-light resonance frequency shift $\Delta\nu$ in a Cartesian coordinate system $(t, \Delta\nu)$ has the form of parallel slant lines [184].

Input resonances are induced if condition (16) for the incident light frequency is fulfilled, leading to an increase of energy density in the droplet and a proportional rise in the RS cross section. Taken together, these changes result in an enhancement of RS efficiency over the entire frequency range. This explains why the time dependence $\Delta\nu(t)$ is depicted by vertical lines in a Cartesian coordinate system [184]. Input resonances are responsible for well-apparent narrow peaks in the frequency dependence of the RS cross section integrated over a wide frequency interval. Also, the majority of input resonances are observed in the elastic light scattering spectrum. However, some input resonances in the Mie scattering spectrum are liable to reduce owing to the light pressure that acts on the droplet [199].

In paper [184], Raman and elastic scattering of light was examined in an inhomogeneous droplet composed of two immiscible fluids — a glycerol core and a thin surface layer of dioctyl phthalate. The optical diagnostic technique employed in Ref. [184] demonstrated that the core of the droplet evaporated quicker than a homogeneous glycerol droplet. A similar result was obtained in an earlier work [200] based on the measurements of the Mie scattering cross section. Also, elastic scattering of light by a two-layer sphere was documented in work [201]. The resonant scattering technique was applied to study spectra of suspended microparticles with the shell as thin as a few nanometers [202, 203]. The properties of structural resonances in internal and scattered light intensities in coated spheres were considered in Refs [204 – 206]. All these studies were liable to use a theoretical model [207] which extended the Lorenz – Mie theory to the light scattering in a double-layer sphere.

In research studies [182,198], inhomogeneous droplets were produced by doping a fluid with polymeric spherical particles with a radius of a few tens of nanometers. These added particles caused additional scattering of light in the fluid and resulted in a significant alteration of the droplets' radiative properties. Specifically, new resonance lines were observed to appear in the fluorescence [198] and Raman [182] scattering spectra, induced by the excitation of lower-Q modes of higher orders.

7. Altered rates of physicochemical processes

Changes of the Einstein coefficients for spontaneous radiation are not the sole effect illustrating the relationship between the process rate and density of photon states. Other physical anomalies can also be expected to occur in droplets. At present, it is known that the rate of energy transfer between dye molecules immersed in a droplet may increase [66, 208 – 211]. A study reported in Ref. [208] demonstrated that the energy transfer between donor and acceptor dye molecules in a droplet is due to the presence of optical WGM if the molecular concentration is low and no ordinary radiationless diffusion of excitation occurs. The experimental findings found a fairly convincing theoretical explanation in paper [210] which considers the process as going through two stages. At the first stage, donor dye molecules emit light into whispering gallery modes. The second step involves absorption of light circulating inside the droplet by acceptor molecules.

Formalism developed in work [61] permits the examination of changes in spectral density of thermal radiation $S(\omega, T)$ emitted by microdroplets in equilibrium with the surrounding medium. Indeed, the quantity $S(\omega, T)$ (defined as the energy radiated into a unit interval of frequency ω at ball temperature T) is proportional to the density of states (12):

$$S(\omega, T) = \rho^{C}(\omega)\, W(\omega, T)\,, \tag{18}$$

where the average energy $W(\omega, T)$ of the mode is given by the Planck distribution

$$W(\omega, T) = \hbar\omega \left(\exp\frac{\hbar\omega}{k_B T} - 1 \right)^{-1}.$$

Here k_B is the Boltzmann constant. The ratio of $S(\omega, T)$ to the Planck radiation density of a blackbody of volume V, viz.

$$S_P(\omega, T) = \rho_v(\omega)\, V\, W(\omega, T)\,,$$

is given by

$$\frac{S(\omega, T)}{S_P(\omega, T)} = G(x, n)\,.$$

It follows from Fig. 2 that the factor G as a function of x may exhibit sharp peaks with an amplitude of up to 100.

A theoretical consideration of the thermal radiation transfer in a microdroplet was presented by Lange and Schweiger [212]. The model is based on a RS theory in which the intensity of the dipole radiation in a dielectric ball is computed in the framework of classical electrodynamics [72 – 74]. According to the authors of paper [212], the thermal radiation from a ball is produced by an assemblage of cells into which it can be divided, each emitting dipole radiation. The radiated power of an individual cell $P_P(r, \omega/c)$ was averaged over dipole orientations. Light absorption by the ball was allowed for by reference to the imaginary part of its refractive index. Lange and Schweiger [212] first considered the properties of a microdroplet with the dipole oscillation amplitude being unrelated to the dipole location inside the droplet, i.e. at constant T. It was shown that this approximation led to the rederivation of Kirchhoff's law in accordance with which the thermal radiation power of a body in thermal equilibrium is equal to the radiation power absorbed by this body. Thereafter, the model was generalized to the case of an arbitrary temperature distribution. It predicted anomalous dependences of both the amplitude and angular distribution of thermal radiation, arising from WGM excitation. To be exact, a periodic structure induced by the ball's action as a resonator was superimposed on the Planck distribution of thermal radiation power. In particular, in the dependence of P_P on the wave number $k = \omega/c$ in the center of the particle ($r = 0$), equidistant maxima were visible produced by the excitation of radial standing waves of TE polarization. The distance between two adjacent maxima was approximately π/a. In the vicinity of the droplet's surface ($r \geqslant 0.8a$), a periodic structure was caused by an excitation of WGM. At $r = 0.4a$, neither WGM nor radial standing waves were excited and could therefore be neglected. Under these conditions, the dependence $P_p(\omega, k)$ did not significantly deviate from the Planck distribution.

Gel'mukhanov and Shalagin [213] theoretically predicted the phenomenon of light-induced diffusion (LID) of gases, consisting in that a gas showing resonance absorption upon the transition from the ground state can travel with a macroscopic speed in the direction of a light beam or against it. LID is known to take place only in a traveling wave field; it does not occur in a standing wave field [213 – 215]. However, this observation appears to be true of homogeneous systems alone. In inhomogeneous systems, LID must manifest itself in a nontrivial way. A study of light scattering from droplets irradiated in a gas mixture has shown [216] that it can be regarded as a conversion of the standing wave field to traveling waves propagating apart from the droplet. Such waves can trigger a light-induced molecular drift which can be oriented either towards the droplet or in the opposite direction by frequency tuning. The light-induced growth (evaporation) of the droplets is described by a system of equations for LID taking into consideration spatial inhomogeneity and diffusion flows [213 – 215]. A very complicated solution of this system was found in paper [216]; it includes numerical estimates of the light-induced droplet growth rate. For example, it is demonstrated that, owing to LID, the droplets of approximately 10 μm in size, spaced at 1 mm, can absorb all vapor for 0.1 – 1 s. Light frequency tuning can entail light-induced evaporation of droplets leading to their stationary distribution by size due to enhanced vapor tension. Thus, the light-induced instability of droplets in the standing wave field offers a unique opportunity to control their growth or evaporation.

8. Hierarchy of processes inherent in droplet irradiation by high-intense light

Hsieh et al. [217] reviewed the results of experiments in which changes in droplet emissive properties were measured as the incident radiation intensity gradually increased to well above the lasing threshold. These experiments were conducted on rhodamine-doped ethanol droplets with a radius of 35 μm, produced with a Berglund – Liu aerosol generator. The illumination source was designed around the second-harmonic output of a Q-switched neodymium laser ($\lambda = 532$ nm). The intensity of light pulses of about 15-ns duration increased from 100 MW cm^{-2} to 6 GW cm^{-2}.

It was known that the lasing threshold was achievable at a pump intensity of 0.5 W cm^{-2} using continuous radiation from an Ar^+ laser [114], and at 10^4 W cm^{-2} when the second harmonic of a pulsed Nd laser was used as the illumination source [87]. Droplets emitted laser radiation within a broad range of pulse pumping intensities (from 1 to 100 MW cm^{-2}). The radiation spectra exhibited several clusters of equidistant narrow peaks, which suggested lasing on WGM with different indices p, l, q [see Fig. 6 and Eqn (16)].

As the pump intensity increased to 100 MW cm^{-2} and above, broadened peaks of induced radiation in WGM could be observed. Simultaneously, sharp peaks related to the droplet structure disappeared from the spectra. Such broad laser radiation spectra were attributable to the saturation of lasing on WGM with high Q. In parallel, lasing on lower-Q WGM was initiated. It was suggested in paper [218] that the broadening of individual peaks of stimulated radiation might be due to the relationship between the light intensity and refractive index in a fluid. As a result, the laser radiation field inside a droplet may cause a change of oscillation phase with time.

A pumping intensity above 500 MW cm^{-2} resulted in the appearance of stimulated Raman scattering of light. This process shows strong dependence on the droplet-forming fluid and dissolved impurities it contains. SRS as a channel of incident radiation energy dissipation may compete against lasing in droplets [142, 154].

At a pumping light intensity close to 6 GW cm^{-2}, a plasma torch arose outside the shadow face of the droplet. The torch was as long as a few diameters of the droplet. Both the droplet and the plasma torch contributed to continuous radiation which was generated by virtue of recombination processes and radiative transitions between energy levels of electrons, ionized atoms, and electronically excited molecules. Discrete emission lines of atomic hydrogen (H_α, H_β), oxygen and nitrogen ions (O II, N II) were superimposed on the continuous spectrum due to laser-induced ethanol and air decomposition. The formation of electrons, ionized atoms, and

excited molecular states in the plasma torch outside the shadow face of the droplet was initiated by the processes of multiphoton absorption and cascade collisional ionization inside the droplet. The particles thus formed were expelled from the droplet in the direction of the laser beam (by a shock wave or light-supported detonation wave) and later caused an air breakdown behind the droplet's shadow face. Some experimenters were able to observe a plasma torch of lesser size in front of the illuminated side of the droplet.

A series of experiments were designed to study specific effects of high-intense laser radiation on the droplets. For example, Zhang and Chang [219] described conditions in which the force of electrostriction associated with laser irradiation of a droplet was comparable with surface tension forces. Due to this, the droplet assumed the form of a cylinder or ejected a droplet of a smaller radius. Laser-induced breakdown and detonation waves in droplets were studied in experiments [220–226], and explosive vaporization of transparent droplets in papers [227–232].

9. Conclusions

The Mie scattering spectrum of a spherical particle contains resonance electromagnetic modes (the electromagnetic field in a ball is considerably different from that in a homogeneous medium). This accounts for a significant change in the rate of optical processes and may be regarded as the resonance interaction of emitting atoms and molecules with dielectric particles. Indeed, at certain discrete values of the radius of a ball, the probability of spontaneous emission by an excited atom located close to its surface tends to increase by several orders of magnitude. The same is true of other optical processes including nonlinear ones. It is important that, first, microdroplets are characterized by very high quality factors and, second, WGM-filled volumes are small. The combination of these two factors makes it possible to achieve the thresholds of nonlinear optical phenomena at low pump intensities. This explains why the recent years have witnessed so many new optical effects, which it was the aim of the present review to consider.

References

1. Zuev V E, Kopytin Yu D, Kuzikovskiĭ A V *Nelineĭnye Opticheskie Effekty v Aerozolyakh* (Nonlinear Optical Effects in Aerosols) (Novosibirsk: Nauka, 1980)
2. Smirnov B M *Usp. Fiz. Nauk* **160** (4) 1 (1990) [*Sov. Phys. Usp.* **33** 261 (1990)]
3. Corum K L, Corum J F *Usp. Fiz. Nauk* **160** (4) 47 (1990)
4. Smirnov B M *Usp. Fiz. Nauk* **162** (1) 119 (1992) [*Sov. Phys. Usp.* **35** 37 (1992)]
5. Smirnov B M *Usp. Fiz. Nauk* **162** (8) 43 (1992) [*Sov. Phys. Usp.* **35** 650 (1992)]
6. Vasil'eva I A *Usp. Fiz. Nauk* **163** (8) 47 (1993) [*Phys. Usp.* **36** 694 (1993)]
7. Smirnov B M *Usp. Fiz. Nauk* **163** (10) 29 (1993) [*Phys. Usp.* **36** 933 (1993)]
8. Smirnov B M *Usp. Fiz. Nauk* **164** 665 (1994) [*Phys. Usp.* **37** 621 (1994)]
9. Smirnov B M *Usp. Fiz. Nauk* **164** 1165 (1994) [*Phys. Usp.* **37** 1079 (1994)]
10. Eletskiĭ A V, Smirnov B M *Usp. Fiz. Nauk* **166** 1197 (1996) [*Phys. Usp.* **39** 1137 (1996)]
11. Smirnov B M *Usp. Fiz. Nauk* **167** 1169 (1997) [*Phys. Usp.* **40** 1117 (1997)]
12. Smirnov B M *Usp. Fiz. Nauk* **170** 495 (2000) [*Phys. Usp.* **43** 453 (2000)]
13. Konyukhov V K, Faĭzullaev V N *Kvantovaya Elektron.* **1** 2623 (1974)
14. Gordiets B F, Shelepin L A, Shmotkin Yu S *Fiz. Goreniya Vzryva* **18** 71 (1982)
15. Oraevskiĭ A N, Protsenko I E *Pis'ma Zh. Eksp. Teor. Fiz.* **72** 641 (2000) [*JETP Lett.* **72** 445 (2000)]
16. Descartes R *Dioptrique* (Leiden, 1639); *Discourse on Method, Optics, Geometry and Meteorology* (Indianapolis: Bobbs-Merrill, 1965)
17. Airy G B *Trans. Cambridge Philos. Soc.* **6** 379 (1838)
18. Wang R T, van de Hulst H C *Appl. Opt.* **30** 106 (1991)
19. Descartes R *Géométrie* (Leyden: De Limprimerie de I Maire, 1637) [Translated into English: *Geometry* (New York: Dover Publ., 1954)]
20. Ungut A, Grehan G, Goesbet G *Appl. Opt.* **20** 2911 (1981)
21. Glantschnig W J, Chen S H *Appl. Opt.* **20** 2499 (1981)
22. Lock J A *Appl. Opt.* **35** 500 (1996)
23. Muinonen K et al. *J. Quant. Spectrosc. Radiat. Trans.* **55** 577 (1996)
24. Velesco N, Kaiser T, Schweiger G *Appl. Opt.* **36** 8724 (1997)
25. Roll G et al. *J. Opt. Soc. Am. A* **15** 2879 (1998)
26. Roll G, Kaiser T, Schweiger G *J. Opt. Soc. Am. A* **16** 882 (1999)
27. Velesco N, Schweiger G *Appl. Opt.* **38** 1046 (1999)
28. Lorenz L V *Vidensk. Selsk. Shrifter* **6** 1 (1890)
29. Mie G *Ann. Phys.* (Leipzig) **25** 377 (1908)
30. Debye P *Ann. Phys.* (Leipzig) **30** 57 (1909)
31. Love A E *Proc. Lond. Math. Soc.* **30** 308 (1899)
32. van de Hulst H *Optics of Spherical Particles* (Amsterdam: Drukkerij J.F. Duwaer, 1946) [Translated into Russian (Moscow: IL, 1961)]
33. Kerker M *The Scattering of Light, and Other Electromagnetic Radiation* (New York: Academic Press, 1969)
34. Lord Rayleigh J W *Philos. Mag.* **20** 1001 (1910)
35. Braginskiĭ V B, Il'chenko V S *Dokl. Akad. Nauk SSSR* **293** 1358 (1987)
36. Braginskiĭ V B, Il'chenko V S, Gorodetskiĭ M L *Usp. Fiz. Nauk* **160** 157 (1990) [*Sov. Phys. Usp.* **33** 83 (1990)]
37. Braginsky V B, Gorodetsky M L, Ilchenko V S *Phys. Lett. A* **137** 393 (1993)
38. Ilchenko V S, Gorodetsky M L, Vyatchanin S P *Opt. Commun.* **107** 41 (1994)
39. Gorodetsky M L, Il'chenko V S *Opt. Commun.* **113** 133 (1994)
40. Gorodetsky M L, Savchenkov A A, Ilchenko V S *Opt. Lett.* **21** 453 (1996)
41. Oraevsky A N, Bandy D K *Opt. Commun.* **129** 75 (1996)
42. Klimov V V, Ducloy M, Letokhov V S *J. Mod. Opt.* **44** 1081 (1997)
43. Klimov V V, Letokhov V S, Ducloy M *Phys. Rev. A* **56** 2308 (1997)
44. Oraevskiĭ A N, Scully M, Vlichanskiĭ V L *Kvantovaya Elektron.* **25** 211 (1998) [*Quantum Electron.* **28** 203 (1998)]
45. Rayleigh J W *Philos. Mag.* **41** 107, 274, 447 (1871)
46. Born M, Wolf E *Principles of Optics* (Oxford: Pergamon Press, 1968) [Translated into Russian (Moscow: Nauka, 1973)]
47. Vaĭnshteĭn L A *Otkrytye Rezonatory i Otkrytye Volnovody* (Open Resonators and Open Waveguides) (Moscow: Sov. Radio, 1966) [Translated into English (Boulder, Colo.: Golem Press, 1969)]
48. Shifrin K S, Zolotov I G *Appl. Opt.* **32** 5397 (1993)
49. Chýlek P, Kiehl J T, Ko M K W *Appl. Opt.* **17** 3019 (1978)
50. Perelman A Y *Appl. Opt.* **30** 475 (1991)
51. Kaup D J *Phys. Rev. A* **41** 5092 (1990)
52. Chýlek P *J. Opt. Soc. Am.* **66** 285 (1976)
53. Datsyuk V V, Izmaĭlov I A, Kochelap V A *Kvantovaya Elektron.* (Kiev) **38** 56 (1990)
54. Chýlek P *J. Opt. Soc. Am. A* **7** 1609 (1990)
55. Schiller S, Byer R L *Opt. Lett.* **16** 1138 (1991)
56. Datsyuk V V *Appl. Phys. B* **54** 184 (1992)
57. Lam C C, Leung P T, Young K *J. Opt. Soc. Am. B* **9** 1585 (1992)
58. Schiller S *Appl. Opt.* **32** 2181 (1993)
59. Johnson B R *J. Opt. Soc. Am. A* **10** 343 (1993)
60. Purcell E M *Phys. Rev.* **69** 681 (1946)
61. Ching S C, Lai H M, Young K *J. Opt. Soc. Am. B* **4** 1995 (1987)
62. Ching S C, Lai H M, Young K *J. Opt. Soc. Am. B* **4** 2004 (1987)
63. Lai H M, Leung P T, Young K *Phys. Rev. A* **37** 1597 (1988)
64. Campillo A J, Eversole J D, Lin H-B *Phys. Rev. Lett.* **67** 437 (1991)
65. Lin H-B et al. *Phys. Rev. A* **45** 6756 (1992)
66. Campillo A J, Eversole J D, Lin H-B *Mod. Phys. Lett. B* **6** 447 (1992)

67. Vlasenko N A, Pekar S I, Pekar V S *Zh. Eksp. Teor. Fiz.* **64** 371 (1973) [*Sov. Phys. JETP* **37** 223 (1973)]
68. Pekar V S *Zh. Eksp. Teor. Fiz.* **67** 471 (1974) [*Sov. Phys. JETP* **40** 236 (1975)]
69. Pekar V S *Ukr. Fiz. Zh.* **19** 1351 (1974)
70. Chew H *J. Chem. Phys.* **87** 1355 (1987)
71. Chew H *Phys. Rev. A* **38** 3410 (1988)
72. Chew H, McNulty P J, Kerker M *Phys. Rev. A* **13** 396 (1976)
73. Kerker M et al. *J. Opt. Soc. Am.* **68** 1676 (1978)
74. Chew H et al. *J. Opt. Soc. Am.* **68** 1686 (1978)
75. Kerker M, Druger S D *Appl. Opt.* **18** 1172 (1979)
76. Serpengüzel A et al. *Appl. Opt.* **31** 3543 (1992)
77. Ashkin A, Dziedzic J M *Phys. Rev. Lett.* **38** 1351 (1977)
78. Chýlek P *Phys. Rev. A* **18** 2229 (1978)
79. Benner R E et al. *Phys. Rev. Lett.* **44** 475 (1980)
80. Owen J F, Chang R K, Barber P W *Aerosol Sci. Technol.* **1** 293 (1982)
81. Conwell P R, Barber P W, Rushfort C K *J. Opt. Soc. Am. A* **1** 62 (1984)
82. Chýlek P, Pendleton J D, Pinnick R G *Appl. Opt.* **24** 3940 (1985)
83. Hill S C, Benner R E *J. Opt. Soc. Am. B* **3** 1509 (1986)
84. Chang R K, in *Advances in Laser Science – II* (AIP Conf. Proc., Vol. 160, Eds M Lapp, W C Stwalley, G A Kenney-Wallace) (New York: AIP, 1987) p. 509
85. Chýlek P et al. *Opt. Lett.* **16** 1723 (1991)
86. Esen C, Schweiger G *Chem. Sci. Technol.* **21** 36 (1998)
87. Lin H B et al. *J. Opt. Soc. Am. B* **8** 250 (1986)
88. Lai H M et al. *Phys. Rev. A* **41** 5187 (1990)
89. Lai H M, Leung P T, Young K *Phys. Rev. A* **41** 5199 (1990)
90. Lai H M et al. *J. Opt. Soc. Am. B* **8** 1962 (1991)
91. Chen G et al. *Opt. Lett.* **16** 1269 (1991)
92. Chen G, Swindal J C, Chang R K *Proc. SPIE* **1726** 292 (1992)
93. Chen G et al. *Proc. SPIE* **1862** 200 (1993)
94. Chen G et al. *Opt. Lett.* **18** 1993 (1993)
95. Guker F T, Egan E E *J. Colloid Sci.* **16** 68 (1961)
96. Davis E J, in *Surface Colloidal Sci.* Vol. 14 (Ed. E Matijevic) (New York: Plenum Press, 1987)
97. Ray A K et al. *Appl. Opt.* **30** 3974 (1991)
98. Devarakonda V et al. *Aerosol Sci. Technol.* **28** 531 (1998)
99. Swindal J C et al., in *Recent Advances in Spray Combustion* (AIAA Progress Series, Vol. 171, Ed. K K Kuo) (Washington, D.C.: AIAA, 1995) p. 63
100. Tolpygo K B, Chalyĭ A V *Zh. Prikl. Spektrosk.* **2** 167 (1965)
101. Tolpygo K B, Chalyĭ A V *Zh. Prikl. Spektrosk.* **2** 447 (1965)
102. Chaly A V *Zh. Prikl. Spektrosk.* **4** 162 (1966)
103. Chaly A V *Ukr. Fiz. Zh.* **11** 50 (1966)
104. Weber R, Schweiger G *J. Colloid Interf. Sci.* **210** 86 (1999)
105. Holt R G, Crum L A *Appl. Opt.* **29** 4182 (1990)
106. Lord Rayleigh J W *Philos. Mag.* **34** 94 (1917)
107. Zel'dovich Ya B, Raĭzer Yu P *Fizika Udarnykh Voln i Vysokotemperaturnykh Gidrodinamicheskikh Yavleniĭ* (Physics of Shock Waves and High-Temperature Hydrodynamic Phenomena) (Moscow: Nauka, 1966) [Translated into English (New York: Academic Press, 1966)]
108. Margulis M A *Usp. Fiz. Nauk* **170** 263 (2000) [*Phys. Usp.* **43** 259 (2000)]
109. Tzeng H-M et al. *Opt. Lett.* **8** 273 (1984)
110. Tzeng H-M et al. *Proc. SPIE* **573** 80 (1985)
111. Hill S C et al. *Appl. Opt.* **24** 2380 (1985)
112. Qian S-X et al. *Science* **231** 486 (1986)
113. Tzeng H-M et al. *Opt. Lett.* **10** 209 (1985)
114. Tzeng H-M et al. *Opt. Lett.* **9** 499 (1984)
115. Eversole J D, Lin H-B, Campillo A J *Appl. Opt.* **31** 1982 (1992)
116. Bykovskiĭ Yu A et al. *Kvantovaya Elektron.* **2** 1803 (1975)
117. Bykovskiĭ Yu A et al. *Zh. Prikl. Spektrosk.* **23** 866 (1975)
118. Rosasco G J, Etz E S, Cassatt W A *Appl. Spectrosc.* **29** 396 (1975)
119. Thurn R, Kiefer W *J. Raman. Spectrosc.* **15** 411 (1984)
120. Thurn R, Kiefer W *Appl. Spectrosc.* **38** 78 (1984)
121. Thurn R, Kiefer W *Appl. Opt.* **24** 1515 (1985)
122. Lettieri T R, Preston R E *Opt. Commun.* **54** 349 (1985)
123. Fung K H, Tang I N *Appl. Opt.* **27** 206 (1988)
124. Fung K H, Tang I N *Chem. Phys. Lett.* **147** 509 (1988)
125. Fung K H, Tang I N *J. Colloid Interf. Sci.* **130** 219 (1989)
126. Tang I N, Fung K H *J. Aerosol Sci.* **20** 609 (1989)
127. Fung K H, Tang I N *Chem. Phys. Lett.* **163** 560 (1989)
128. Lord Rayleigh J W *Philos. Mag.* **14** 184 (1882)
129. Feng J Q, Beard K V *Proc. R. Soc. London Ser. A* **430** 133 (1990)
130. Snow J B, Qian S-X, Chang R K *Opt. Lett.* **10** 37 (1985)
131. Qian S-X, Snow J B, Chang R K, in *Laser Spectroscopy VII* (Springer Series in Optical Sciences, Vol. 49, Eds T W Hänsch, Y R Shen) (Berlin: Springer-Verlag, 1985) p. 204
132. Qian S-X, Snow J B, Chang R K *Opt. Lett.* **10** 499 (1985)
133. Snow J B, Qian S-X, Chang R K *Opt. News* **12** 5 (1986)
134. Qian S-X, Chang R K *Phys. Rev. Lett.* **56** 926 (1986)
135. Eickmans J H, Qian S-X, Chang R K *Part. Charact.* **4** 85 (1987)
136. Zhang J-Z, Leach D H, Chang R K *Opt. Lett.* **13** 270 (1988)
137. McNulty P J, Chew H W, Kerker M, in *Aerosol Microphysics I: Particle Interaction* (Topics in Current Physics, Vol. 16, Ed. W H Marlow) (Berlin: Springer-Verlag, 1980)
138. Kerker M *Aerosol Sci. Technol.* **1** 275 (1982)
139. Chan K, Flagan R C, Seinfeld J H *Appl. Opt.* **30** 459 (1991)
140. Lange S, Schweiger G *J. Opt. Soc. Am. B* **13** 1864 (1996)
141. Latifi H et al. *Appl. Opt.* **29** 5387 (1990)
142. Kwok A S, Chang R K *Opt. Lett.* **18** 1597 (1993)
143. Chang R K, in *Laser Optics of Condensed Matter: Proc. Third USA-USSR Symposium, 1987, USSR* (Eds J L Birman, H Z Cummins, A A Kaplyanskii) (New York: Plenum Press, 1988) p. 193
144. Biswas A et al. *Phys. Rev. A* **40** 7413 (1989)
145. Lin H-B, Eversole J D, Campillo A J *Opt. Commun.* **77** 407 (1990)
146. Lin H-B et al. *J. Opt. Soc. Am. B* **7** 2079 (1990)
147. Serpengüzel A, Chen G, Chang R K *Part. Sci. Technol.* **8** 179 (1990)
148. Chen G et al. *Opt. Lett.* **16** 117 (1991)
149. Chang R K et al. *Proc. SPIE* **1497** 2 (1991)
150. Lin H B, Eversole J D, Campillo A J *Opt. Lett.* **17** 828 (1992)
151. Lange S, Schweiger G *J. Opt. Soc. Am. B* **14** 1931 (1997)
152. Chang R K, Qian S-X, Eickmans J, in *Methods of Laser Spectroscopy* (Eds Y Prior, A Ben-Reuven, M Rosenbluth) (New York: Plenum Press, 1986) p. 249
153. Leach D H, Chang R K, Acker W P *Opt. Lett.* **17** 387 (1992)
154. Kwok A S, Chang R K *Opt. Lett.* **18** 1703 (1993)
155. Hsieh W-F, Zheng J-B, Chang R K *Opt. Lett.* **13** 497 (1988)
156. Zheng J-B et al., in *Proc. Topical Meeting on Laser Materials and Laser Spectroscopy, 1988, China* (Eds Z Wang, Z Zhang) (Singapore: World Scientific, 1989) p. 259
157. Serpengüzel A et al. *J. Opt. Soc. Am. B* **9** 871 (1992)
158. Zhang J-Z, Chang R K *J. Opt. Soc. Am. B* **6** 151 (1989)
159. Zhang J-Z, Chen G, Chang R K *J. Opt. Soc. Am. B* **7** 108 (1990)
160. Wirth F H et al. *Opt. Lett.* **17** 1334 (1992)
161. Acker W P, Leach D H, Chang R K *Opt. Lett.* **14** 402 (1989)
162. Leach D H, Acker W P, Chang R K *Opt. Lett.* **15** 894 (1990)
163. Qian S-X et al. *Opt. Commun.* **74** 414 (1990)
164. Chang R K, in *Resonances* (Eds M D Levenson et al.) (Singapore: World Scientific, 1990) p. 200
165. Qian S-X, Wang J, Li Y *Chinese Phys. Lett.* **5** 205 (1988)
166. Carls J C, Moncivais G, Brock J R *Appl. Opt.* **29** 2913 (1990)
167. Acker W P et al. *Appl. Phys. B* **51** 9 (1990)
168. Zhu J, Dunn-Rankin D *Appl. Opt.* **30** 2672 (1991)
169. Tang I N et al. *Aerosol Sci. Technol.* **23** 443 (1995)
170. Vehring R et al. *J. Aerosol Sci.* **29** 1045 (1998)
171. Schweiger G *J. Aerosol Sci.* **21** 483 (1990)
172. Fung K H, Tang I N *Appl. Spectrosc.* **45** 734 (1991)
173. Fung K H, Tang I N *Appl. Spectrosc.* **46** 1189 (1992)
174. Fung K H, Imre D G, Tang I N *J. Aerosol Sci.* **25** 479 (1994)
175. Vehring R et al. *Rev. Sci. Instrum.* **68** 70 (1997)
176. Davis E J, Buehler M F, Ward T L *Rev. Sci. Instrum.* **61** 1281 (1990)
177. Buehler M F, Allen T M, Davis E J *J. Colloid Interf. Sci.* **146** 79 (1991)
178. Schweiger G *J. Opt. Soc. Am. B* **8** 1770 (1991)
179. Foss W et al. *Aerosol Sci. Technol.* **18** 187 (1993)
180. Schaschek K, Popp J, Kiefer W *Ber. Bunsen. Phys. Chem.* **97** 1007 (1993)
181. Schaschek K, Popp J, Kiefer W *J. Raman Spectrosc.* **24** 69 (1993)
182. Kaiser T, Roll G, Schweiger G *J. Opt. Soc. Am. B* **12** 281 (1995)
183. Kaiser T et al. *Ber. Bunsen. Phys. Chem.* **100** 119 (1996)
184. Kaiser T, Roll G, Schweiger G *Appl. Opt.* **35** 5918 (1996)
185. Popp J et al. *Appl. Opt.* **34** 2380 (1995)

186. Popp J et al. *J. Mol. Struct.* **348** 281 (1995)
187. Aardahl C L, Foss W F, Davis E J *J. Aerosol Sci.* **27** 1015 (1996)
188. Aardahl C L, Foss W F, Davis E J *Indian. Eng. Chem. Res.* **35** 2834 (1996)
189. Rassat S D, Davis E J *J. Aerosol Sci.* **23** 165 (1992)
190. Buehler M F, Davis E J *Colloid Surf. A* **79** 137 (1993)
191. Li W et al. *J. Colloid Interf. Sci.* **162** 267 (1994)
192. Aardahl C L, Davis E J *Mater. Res. Soc. Symp. Proc.* **432** 209 (1996)
193. Aardahl C L, Davis E J *Appl. Spectrosc.* **50** 71 (1996)
194. Essen C, Kaiser T, Schweiger G *Appl. Spectrosc.* **50** 823 (1996)
195. Essen C et al. *Colloid Polym. Sci.* **275** 131 (1997)
196. Schweiger G *Opt. Lett.* **15** 156 (1990)
197. Eversole J D, Lin H-B, Campillo A J *J. Opt. Soc. Am. B* **12** 287 (1995)
198. Lin H-B et al. *Opt. Lett.* **17** 970 (1992)
199. Schweiger G *J. Opt. Soc. Am. B* **8** 174 (1991)
200. Ray A K et al. *Langmuir* **7** 525 (1991)
201. Hightower R L et al. *Opt. Lett.* **13** 946 (1988)
202. Huckaby J L, Ray A K *Langmuir* **11** 80 (1995)
203. Ray A K, Nandakumar R *Appl. Opt.* **34** 7759 (1995)
204. Hightower R L, Richardson C B *Appl. Opt.* **27** 4850 (1988)
205. Lock J A *Appl. Opt.* **29** 3180 (1990)
206. Kaiser T, Lange S, Schweiger G *Appl. Opt.* **33** 7789 (1994)
207. Aden A L, Kerker M *J. Appl. Phys.* **22** 1242 (1951)
208. Folan L M, Arnold S, Druger S D *Chem. Phys. Lett.* **118** 322 (1985)
209. Druger S D, Arnold S, Folan L M *J. Chem. Phys.* **87** 2649 (1987)
210. Leung P T, Young K *J. Chem. Phys.* **89** 2894 (1988)
211. Arnold S, Folan L M *Opt. Lett.* **14** 387 (1989)
212. Lange S, Schweiger G *J. Opt. Soc. Am. B* **11** 2444 (1994)
213. Gel'mukhanov F Kh, Shalagin A M *Zh. Eksp. Teor. Fiz.* **77** 461 (1979) [*Sov. Phys. JETP* **50** 238 (1979)]
214. Gel'mukhanov F Kh, Shalagin A M *Zh. Eksp. Teor. Fiz.* **78** 1672 (1980) [*Sov. Phys. JETP* **51** 877 (1980)]
215. Antsygin V D, in *Nelineĭnaya Optika. Trudy VI Vavilovskoĭ Konferentsii.* Ch. II (Non-Linear Optics. Proceedings VI Vavilov Conference) Part II (Ed. V P Chebotaev) (Novosibirsk: Inst. Teplofiziki SO AN SSSR, 1979) p. 159
216. Kalechits V I, Nakhutin I E, Poluektov P P *Kvantovaya Elektron.* **9** 1518 (1982)
217. Hsieh W-F, Tzeng H-M, Chang R K *Acad. Sinica* **16** 1 (1986)
218. Qian S-X, Chang R K *Opt. Lett.* **11** 371 (1986)
219. Zhang J Z, Chang R K *Opt. Lett.* **13** 916 (1988)
220. Chang R K et al. *Appl. Opt.* **27** 2377 (1988)
221. Hsieh W-H et al. *Opt. Lett.* **12** 576 (1987)
222. Hsieh W-H, Eickmans J H, Chang R K *J. Opt. Soc. Am. B* **4** 1816 (1987)
223. Eickmans J H, Hsieh W-H, Chang R K *Appl. Opt.* **26** 3721 (1987)
224. Zheng J-B et al. *Opt. Lett.* **13** 559 (1988)
225. Hsieh W-F, Zheng J-B, Chang R K *Opt. Lett.* **14** 1014 (1989)
226. Zheng J-B et al. *J. Opt. Soc. Am. B* **8** 319 (1991)
227. Eickmans J H, Hsieh W-H, Chang R K *Opt. Lett.* **12** 22 (1987)
228. Kuzikovskiĭ A V, Pogodaev V A, Khmelevtsov S S *Inzh.-Fiz. Zh.* **20** 21 (1971)
229. Kostin V A et al. *Zh. Eksp. Teor. Fiz.* **66** 1970 (1974) [*Sov. Phys. JETP* **39** 901 (1974)]
230. Zhang J-Z et al. *Appl. Opt.* **26** 4731 (1987)
231. Wood C F et al. *Appl. Opt.* **27** 2279 (1988)
232. Kwok A S, Wood C F, Chang R K *Opt. Lett.* **15** 664 (1990)